Estimating Regions of Attraction for Transitional Flows Using Quadratic Constraints

Aniketh Kalur, Talha Mushtaq, Peter Seiler, and Maziar S. Hemati, *Member, IEEE*

***Abstract*—This letter describes a method for estimating regions of attraction and bounds on permissible perturbation amplitudes in nonlinear fluids systems. The proposed approach exploits quadratic constraints between the inputs and outputs of the nonlinearity on elliptical sets. This approach reduces conservatism and improves estimates for regions of attraction and bounds on permissible perturbation amplitudes over related methods that employ quadratic constraints on spherical sets. We present and investigate two algorithms for performing the analysis: an iterative method that refines the analysis by solving a sequence of semi-definite programs, and another based on solving a generalized eigenvalue problem with lower computational complexity, but at the cost of some precision in the final solution. The proposed algorithms are demonstrated on low-order mechanistic models of transitional flows. We further compare accuracy and computational complexity with analysis based on sum-of-squares optimization and direct-adjoint looping methods.**

***Index Terms*—Region of attraction, transitional fluid flows, quadratic constraints.**

I. Introduction

ENVIRONMENTAL disturbances can cause fluid flows to transition from a low-skin-friction laminar state to a high-skin-friction turbulent state when the Reynolds number (Re) is sufficiently large. Yet, precisely predicting the onset of transition is notoriously difficult, even in the simplest of geometries [1]–[3]. An ability to reliably estimate if and when transition will arise is directly related to the problem of identifying the region of attraction (ROA) of the system. To this end, in this work we investigate systems-theoretic analysis methods for estimating the ROA of a laminar equilibrium flow and for determining associated bounds on permissible perturbation amplitudes for remaining in this ROA.

Manuscript received March 4, 2021; revised May 7, 2021; accepted May 11, 2021. Date of publication May 17, 2021; date of current version June 25, 2021. This work was supported by Army Research Office under Grant W911NF-20-1-0156. The work of Maziar S. Hemati was supported in part by the Air Force Office of Scientific Research under Award FA 9550-19-1-0034, and in part by the National Science Foundation under Grant CBET-1943988. Recommended by Senior Editor C. Prieur. *(Corresponding author: Maziar S. Hemati.)*

Aniketh Kalur, Talha Mushtaq, and Maziar S. Hemati are with the Department of Aerospace Engineering and Mechanics, University of Minnesota, Minneapolis, MN 55455 USA (e-mail: mhemati@umn.edu).

Peter Seiler is with the Department of Electrical Engineering and Computer Science, University of Michigan at Ann Arbor, Ann Arbor, MI 48109 USA.

Digital Object Identifier 10.1109/LCSYS.2021.3081382

Recent efforts for nonlinear stability analysis of the incompressible Navier-Stokes equations (NSE) have exploited a Lur'e decomposition [4] of the system dynamics into a feedback interconnection between the non-normal linear dynamics and quadratic energy-conserving nonlinearity. Such approaches include dissipation inequalities [5], passivity analysis [6], and sum-of-squares (SOS) optimization [7], all of which generalize the classical energy-based methods of hydrodynamic stability theory [1], [8]. Methods for the analysis of systems with quadratic nonlinearities have also been proposed in prior works [9], [10]; however, these methods scale combinatorially with the state dimension, prohibiting their use on high-dimensional fluids systems.

Most recently, a series of studies have proposed exploiting quadratic constraints (QCs) between the inputs and outputs of the nonlinearity to conduct global and local stability analysis with reduced-complexity [11]–[13]. The trade off for this computational expediency is a larger degree of conservatism in estimating the ROA and associated bounds on permissible perturbation amplitudes relative to more computationally demanding methods, such as SOS [7] and direct-adjoint looping (DAL) [3]. The QC formulation in [13] reduces conservatism compared to the approach in [12], but some conservatism remains because of a restriction to spherical sets.

In this work, we generalized the QCs presented in [11], [12], and [13] to arbitrary ellipsoidal sets. As we will show, these new QCs reduce conservatism and improve estimates of both the ROA and the largest permissible perturbation. We propose algorithms for performing this analysis: one is an iterative algorithm that solves a semi-definite program at each iteration to refine the ROA estimate, and the other is based on solving a single generalized eigenvalue problem (GEVP). Using the QCs generalized on ellipsoidal sets, we analyze ROA estimates and the largest permissible perturbation for system stability; the inner estimate of the ROA captures this perturbation. As an example, we will demonstrate our approach on two low-dimensional mechanistic transitional flow models: the 4-state Walleffe-Kim-Hamilton (WKH) model of shear flow [14] and the 9-state model of Couette flow [15]. Finally, we measure the computational run-time and show that the proposed QC method obtains improved estimates over previous QC approaches [12], [13], while reducing computational time over SOS and DAL methods.

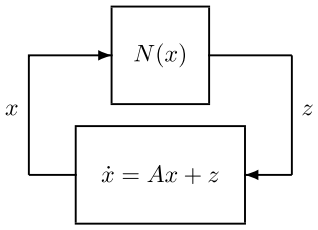

Fig. 1. Lur'e decomposition of nonlinear system.

II. Problem Formulation

Consider a nonlinear system of the following form:

$$\dot{x}(t) = Ax(t) + N(x(t)) \tag{1}$$

where $x(t) \in \mathbb{R}^n$ is the state and the state matrix $A \in \mathbb{R}^{n\times n}$ is Hurwitz. The nonlinearity $N : \mathbb{R}^n \to \mathbb{R}^n$ is assumed to be a quadratic function of the form:

$$N(x) = \begin{bmatrix} x^T Q_1 x \\ \vdots \\ x^T Q_n x \end{bmatrix} \tag{2}$$

where $Q_1, \ldots, Q_n \in \mathbb{R}^{n\times n}$ are symmetric (but not necessarily sign definite) matrices. Moreover, the nonlinearity is assumed to be lossless: $x^T N(x) = 0 \ \forall \ x \in \mathbb{R}^n$. This lossless property is observed in the nonlinear terms of the incompressible NSE and other reduced-order models that mimic transitional flows [15], [16].

It also follows that $N(0) = 0$. Hence $\bar{x} = 0$ is an equilibrium point of the nonlinear system (1). This is an asymptotically stable equilibrium point because A is Hurwitz (see [4, Th. 4.5]). Let $\phi(t, x(0))$ denote the solution of (1) at time t from the initial condition $x(0)$. The region of attraction (ROA) for $\bar{x} = 0$ is defined as:

$$\mathcal{R} := \{x(0) \in \mathbb{R}^n : \phi(t, x(0)) \to 0 \text{ as } t \to \infty\}. \tag{3}$$

In other words, the ROA is the set of initial conditions for which the trajectory asymptotically converges back to the equilibrium point. The equilibrium point $\bar{x} = 0$ is globally asymptotically stable if $\mathcal{R} = \mathbb{R}^n$. In general, the equilibrium point will be locally but not globally asympotitically stable. The objective is to obtain an inner estimate $\hat{\mathcal{R}}$ of the ROA $\mathcal{R}$, i.e., to compute a set $\hat{\mathcal{R}} \subset \mathcal{R}$.

III. Stability Analysis

The stability analysis is based on separating the nonlinearity from the remaining linear dynamics:

$$\dot{x}(t) = Ax(t) + z(t) \tag{4}$$
$$z(t) = N(x(t)). \tag{5}$$

This system can be represented as the Lur'e decomposition [4] as shown in Figure 1.

A. Local Quadratic Constraints

The input-output properties of the nonlinearity can be bounded using a set of QCs on (x, z). The lossless property yields the following global QC:

$$\begin{bmatrix} x \\ z \end{bmatrix}^T \begin{bmatrix} 0 & I \\ I & 0 \end{bmatrix} \begin{bmatrix} x \\ z \end{bmatrix} = 0 \ \ \forall x \in \mathbb{R}^n, z = N(x). \tag{6}$$

To study the effects of nonlinearities locally, additional QCs were formulated in [12] and in [13]. The local QCs in both of these works were defined on a spherical set. In this work, we reduce the conservatism of the aforementioned approaches by generalizing to constraints on an ellipsoidal set. The next lemma generalizes the result in [13] to provide local constraints on an ellipsoidal set.

Lemma 1: Let $E = E^T \succ 0$ be given and define the ellipsoid $\mathcal{E}_\alpha := \{x \in \mathbb{R}^n : x^T E x \le \alpha^2\}$. The nonlinearity N given in (2) satisfies the following local QC for $i = 1, \ldots, n$:

$$\begin{bmatrix} x \\ z \end{bmatrix}^T \begin{bmatrix} \alpha^2 (Q_i E^{-1} Q_i) & 0 \\ 0 & -e_i e_i^T \end{bmatrix} \begin{bmatrix} x \\ z \end{bmatrix} \ge 0, \ \ \forall x \in \mathcal{E}_\alpha, \tag{7}$$

where $e_i \in \mathbb{R}^n$ is the i^{th} standard basis vector.

Proof: Note that $z^T e_i e_i^T z = z_i^2$, where $z_i := x^T Q_i x$ is the i^{th} entry of $z = N(x)$. Define $w := E^{\frac{1}{2}} x$ and $\hat{Q}_i := E^{-\frac{1}{2}} Q_i E^{-\frac{1}{2}}$ so that $z_i = w^T \hat{Q}_i w$. The Cauchy-Schwartz inequality yields the following bound:

$$z_i^2 \le \|w\|_2^2 \cdot \|\hat{Q}_i w\|_2^2. \tag{8}$$

Note that $\|\hat{Q}_i w\|_2^2 = x^T Q_i E^{-1} Q_i x$. Moreover, if $x \in \mathcal{E}_\alpha$ then $\|w\|_2^2 = x^T E x \le \alpha^2$. Combining these facts with Eq. (8) yields $z_i^2 \le x^T [\alpha^2 (Q_i E^{-1} Q_i)] x$ for any $x \in \mathcal{E}_\alpha$. ■

This result corresponds to [13, Lemma 1] for the special case $E = I$. This special case corresponds to a local constraint on a sphere of radius α. The generalization to local constraints on arbitrary ellipsoids will be used to improve our estimates of the ROA.

B. ROA Estimation

We can combine Lyapunov theory with the local QCs from the previous section in order to compute an inner estimate $\hat{\mathcal{R}}$ for the ROA. Roughly, we will define a Lyapunov candidate $V(x) = x^T P x$ and use the QCs to show that $\dot{V}$ is negative definite along the trajectories of Eq. (1) in a neighborhood of the equilibrium point $\bar{x} = 0$. The inner estimate of the ROA will be given by a sphere of radius R, denoted $\hat{\mathcal{R}}_R := \{x \in \mathbb{R}^n : x^T x \le R^2\}$. The next theorem gives a matrix inequality condition to estimate the ROA using local QCs. This is based on a standard Lyapunov result [5, Th. 4.1]. To simplify notation, define the following matrices that appear in the QCs:

$$M_0 := \begin{bmatrix} 0 & I \\ I & 0 \end{bmatrix}, M_i(\alpha, E) := \begin{bmatrix} \alpha^2 (Q_i E^{-1} Q_i) & 0 \\ 0 & -e_i e_i^T \end{bmatrix}. \tag{9}$$

Theorem 1: Let $E = E^T \succ 0$, $\alpha > 0$, $\epsilon > 0$ be given. If $\exists P = P^T \in \mathbb{R}^{n\times n}$, $R > 0$, and $\xi_0, \ldots, \xi_n \in \mathbb{R}$ such that:

$$\begin{bmatrix} A^T P + PA & P \\ P & 0 \end{bmatrix} + \xi_0 M_0 + \sum_{i=1}^{n} \xi_i M_i(\alpha, E) \preceq \begin{bmatrix} -\epsilon I & 0 \\ 0 & 0 \end{bmatrix} \tag{10}$$

$$\frac{1}{\alpha^2} E \preceq P \preceq \frac{1}{R^2} I \tag{11}$$

$$\xi_i \ge 0 \text{ for } i = 1, \ldots, n \tag{12}$$

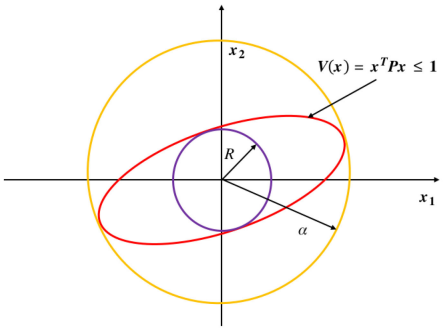

Fig. 2. 2-D visualization of a spherical local region for the QCs corresponding to $E = I$ and $\alpha > 0$ (yellow), Lyapunov function level set $\{x \in \mathbb{R}^n : x^T P x \le 1\}$ (red), and ROA inner estimate $\mathcal{R}_R$ (purple).

then $\hat{\mathcal{R}}_R \subset \mathcal{R}$.

Proof: Define the Lyapunov function $V(x) := x^T P x$. Note that $\frac{1}{\alpha^2} E \preceq P$ implies $P \succ 0$. Multiply (10) on the left/right by $\begin{bmatrix} x(t)^T & z(t)^T \end{bmatrix}$ and its transpose to obtain:

$$\frac{d}{dt} V(x(t)) + \xi_0 \begin{bmatrix} x(t) \\ z(t) \end{bmatrix}^T M_0 \begin{bmatrix} x(t) \\ z(t) \end{bmatrix} + \sum_{i=1}^{n} \xi_i \begin{bmatrix} x(t) \\ z(t) \end{bmatrix}^T M_i \begin{bmatrix} x(t) \\ z(t) \end{bmatrix} \le -\epsilon \|x(t)\|_2^2.$$

The second term with ξ_0 and M_0 is equal to zero due to the global lossless property of $N(x)$. Here, the scalar term ξ_0 can be either positive or negative. While the quadratic terms with ξ_i and M_i ($i = 1$ to n) are each non-negative for any $x(t) \in \mathcal{E}_\alpha$ by Lemma 1 and $\xi_i \ge 0$. Thus $x(t) \in \mathcal{E}_\alpha$ implies $\frac{d}{dt} V(x(t)) \le -\epsilon \|x(t)\|_2^2$.

The constraint $\frac{1}{\alpha^2} E \preceq P$ implies that if $V(x) \le 1$ then $x^T E x \le \alpha^2$, i.e., $\{x \in \mathbb{R}^n : V(x) \le 1\} \subset \mathcal{E}_\alpha$. Hence $\bar{x} = 0$ is locally asymptotically stable and the level set $\{x \in \mathbb{R}^n : V(x) \le 1\}$ is contained in the ROA $\mathcal{R}$ (in [4, Th. 4.1]). Finally, the constraint $P \preceq \frac{1}{R^2} I$ implies that if $x^T x \le R^2$, then $V(x) \le 1$. This yields the desired set containment:

$$\hat{\mathcal{R}}_R \subset \{x \in \mathbb{R}^n : V(x) \le 1\} \subset \mathcal{R}.$$

■

This theorem provides an inner estimate of the ROA characterized by a sphere of radius R. A convex optimization can be used to compute the largest feasible R for given values of (E, α, ϵ). Define $\lambda := \frac{1}{R^2}$ and note that maximizing R is equivalent to minimizing λ. Equations (10)-(12) are linear matrix inequalities (LMIs) in variables (P, ξ, λ). The following optimization is a semidefinite program (SDP):

$$\lambda^* := \min_{P,\xi,\lambda} \lambda \text{ subject to (10)}-\text{(12)}. \tag{13}$$

An SDP is convex and the global optimum λ^* can be computed efficiently using freely available solvers [17], [18]. The radius $R^* = \frac{1}{\sqrt{\lambda^*}}$ provides the largest spherical inner estimate of the ROA for the given local QC region (E, α) and $\epsilon > 0$. The parameter $\epsilon > 0$ is chosen to be a "small" positive number to ensure $\dot{V} < 0$. This term can be dropped if Eq. (10) is feasible with a strict inequality.

The main issue with this numerical method is that it requires the choice of the local QC region in terms of the ellipsoidal shape E and size α. If $E = I$, then the QCs are enforced on a sphere of radius α as shown in Figure 2. A small value of α will restrict the size of both the Lyapunov function level set and the spherical ROA inner estimate. On the other hand, a large value of α may cause the SDP to be infeasible. This occurs because the QC bounds on $N(x)$ become more conservative (less tight) for larger local regions. A one-dimensional line search can be used to compute the best value of α for a given local ellipsoid shape E. For example, the SDP in Eq. (13) can be solved with $E = I$ on a grid of values $\{\alpha_1, \ldots, \alpha_f\}$. Each solution yields an inner ROA estimate with radius $R^*(\alpha_i)$. The best α_i is the one that yields the largest inner ROA estimate: $\max_i R^*(\alpha_i)$.

We can further improve on this inner ROA estimate by exploiting the shape of the ellipsoid as specified by E. Unfortunately Equations (10)-(12) are non-convex in (P, ξ, R, E, α). The first approach, denoted Algorithm 1, iteratively updates the ellipsoid shape based on the Lyapunov function obtained from the previous iterate.

Algorithm 1 : Semi-Definite Program Algorithm for Determining the Largest R^*

1) **Initial Estimate:** Define $M_i(\alpha, E)$ using $E^{(1)} = I$. Find the best $\alpha^{(1)}$ for the given local QCs $E^{(1)}$. Let $(P^{(1)}, \xi^{(1)}, R^{(1)})$ be the corresponding solutions of the SDP with $(E^{(1)}, \alpha^{(1)})$.
2) **Refinement:** Align the local QC set with the Lyapunov function solution: $E^{(2)} = P^{(1)}$. Find the best $\alpha^{(2)}$ for the updated local QCs $E^{(2)}$. Let $(P^{(2)}, \xi^{(2)}, R^{(2)})$ be the corresponding solutions of the SDP with $(E^{(2)}, \alpha^{(2)})$
3) **Iterate:** Repeat the refinement step with $E^{(i+1)} = P^{(i)}$ to yield $(\alpha^{(i)}, P^{(i)}, \xi^{(i)}, R^{(i)})$. This can be performed a fixed number of iterations or until the radius $R^{(i)}$ converges.

The optimal solutions from the first step $(P^{(1)}, \xi^{(1)}, R^{(1)})$ are also feasible for the second step when $\alpha^{(2)} = 1$. The reason is that the constraint $\frac{1}{\alpha^2} E \le P$ in Eq. (11) holds with equality when using $(P, E, \alpha) = (P^{(1)}, P^{(1)}, 1)$. Hence the inner estimate of ROA cannot shrink at the second step: $R^{(2)} \ge R^{(1)}$. Repeating this process gives a monotonically non-decreasing sequence of spherical inner estimates for the ROA: $R^{(i+1)} \ge R^{(i)}$. Note that each step of the iterative method has roughly the same computational cost as the first step. We have to solve one SDP for each value of α_i.

The second approach, denoted Algorithm 2 below, effectively performs only a single refinement of the local shape parameter E. This restriction allows the single refinement step to be formulated as a generalized eigenvalue problem (GEVP) (see [12, eq. (19)]). This will typically reduce the computational cost, but possibly yield more conservative results (smaller estimates for $\hat{\mathcal{R}}_R$) as compared to Algorithm 1. To formulate Algorithm 2, first decompose the quadratic constraint matrix in Eq. (9) into two matrices as follows:

$$M_i(\alpha, E) = \alpha^2 \underbrace{\begin{bmatrix} Q_i E^{-1} Q_i & \mathbf{0} \\ \mathbf{0} & \mathbf{0} \end{bmatrix}}_{M_i^E} + \underbrace{\begin{bmatrix} \mathbf{0} & \mathbf{0} \\ \mathbf{0} & -e_i e_i^T \end{bmatrix}}_{M_i^e}. \tag{14}$$

Algorithm 2 : Generalized Eigenvalue Algorithm for Determining the Largest R^*

1) **Initial Estimate:** Define $M_i(\alpha, E)$ using $E^{(1)} = I$. Find the best $\alpha^{(1)}$ for the given local QCs $E^{(1)}$. Let $(P^{(1)}, \xi^{(1)}, R^{(1)})$ be the corresponding solutions of the SDP with $(E^{(1)}, \alpha^{(1)})$.
2) **Maximize Level Set:** Fix $P = E = P^{(1)}$ and solve the GEVP in Eq. (15) to obtain the maximal level set α^*.
3) **Maximize ROA Inner Estimate:** Select $R^* = \frac{\alpha^*}{\sqrt{\lambda_{max}(P^{(1)})}}$.

Algorithm 2 fixes both the shape $E = P^{(1)}$ and Lyapunov function $P = P^{(1)}$. This aligns both the local QC ellipsoid shape E with the level sets of the Lyapunov function. The local regions for both are parameterized as $\{x \in \mathbb{R}^n : x^T P^{(1)} x \leq \alpha\}$. A sub-problem is to find the largest local region α over which the local quadratic constraints are valid and $\dot{V}(x(t)) < 0$. This is formulated by the following optimization:

$$\begin{aligned} &\min_{\gamma, \xi_0, \ldots, \xi_n} \quad \gamma \\ &\text{subject to} \quad \xi_i \geq 0 \qquad (\text{for } i = 1 \text{ to } n) \\ &\begin{bmatrix} A^T P + PA & P \\ P & \mathbf{0} \end{bmatrix} + \xi_0 M_0 + \sum_{i=1}^{n} \xi_i M_i^e \prec \gamma \sum_{i=1}^{n} \xi_i M_i^E, \quad (15) \end{aligned}$$

where $\gamma = -\alpha^2$ and ξ_i ($i = 0$ to n) are Lagrange multipliers for the global and local constraints respectively. It is emphasized that $P = P^{(1)}$ is fixed and not a decision variable in the optimization. This is a GEVP [19] in variables α^2, $\xi_0, \ldots, \xi_n$. This one GEVP gives the largest level set α^* defined by $P = P^{(1)}$ over which the local quadratic constraints are valid and $\dot{V}(x(t)) < 0$. Let $\lambda_{max}(P^{(1)})$ denote the largest eigenvalue of $P^{(1)}$. Note that the sphere $\hat{\mathcal{R}}_R$ is contained in $\{x \in \mathbb{R}^n : x^T P^{(1)} x \leq \alpha^{*2}\}$ if and only if $R \leq \frac{\alpha^*}{\sqrt{\lambda_{max}(P^{(1)})}}$. Thus we can directly compute the largest radius of the inner ROA estimate $\hat{\mathcal{R}}_R$ from the optimal α^*. This leads to our second method to estimate the ROA.

As a test, we apply algorithm 1 on the 2-D example in [10]. We obtain an inner approximation for the ROA of $R^* = 2.6877$ while [10] reports a box of $[-1, 1] \times [-2, 2]$. Our disk and the box have areas of 22.69 and 8.00, respectively.

IV. Numerical Example

We evaluate the proposed analysis methods on two low-order mechanistic models of transitional flows that were used to demonstrate the QC analysis method in [13]: the 4-state Waleffe-Kim-Hamilton (WKH) model [16] and the 9-state reduced-order model of a plane Couette flow [15]. Both models have the form in Eq. (1), with non-normal linear dynamics and a quadratic lossless nonlinearity. We note that the linear dynamics' matrix is parameterized by the Reynolds number Re: i.e., $A = A(Re)$. Additional details on the specific models used here can be found in [13].

We begin by using the GEVP in Eq. (15) to estimate the size α^* of the ROA over a range of Re. This is done by applying steps 1 and 2 of Algorithm 2. Figures 3(a) and 3(b) show the results of this analysis (light blue) for the WKH and 9-state

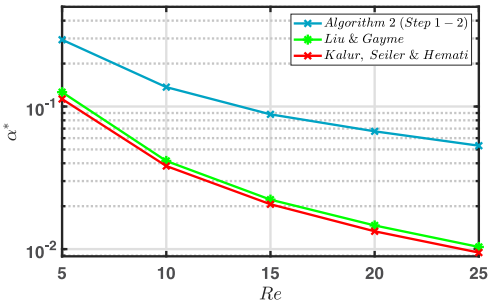

(a) WKH Model

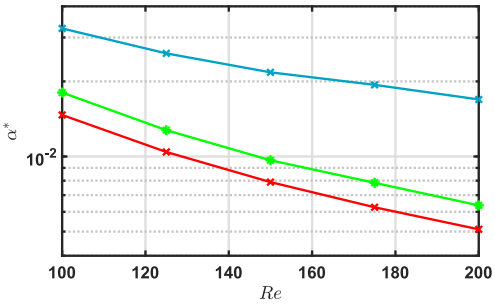

(b) 9-state Couette Flow Model

Fig. 3. The ellipsoidal constraints using step 1 and 2 of algorithm 2 shows significant improvement in region of attraction (ROA) estimates.

Couette flow models, respectively. These results are compared against ROA estimates based on the quadratic constraints proposed in Liu and Gayme [13] (green) and those proposed in Kalur *et al.* [12] (red). This comparison indicates that the ROA estimate based on refinement of the local QC region in steps 1 and 2 of Algorithm 2 leads to less conservative estimates on α^*. Of note here is that although the Liu and Gayme analysis reduces the conservatism in the analysis relative to the Kalur *et al.* analysis, the formulation based on ellipsoidal sets reduces conservatism relative to both of these methods by a substantially larger degree for both mechanistic models.

Next, we apply Algorithm 1 and Algorithm 2 to estimate the inner approximation R^* as a function of Re. This analysis is equivalent to computing a bound on the permissible perturbation amplitude, or sphere of "safe" initial conditions. In Figure 4, the radius of the largest $\hat{\mathcal{R}}_R$ is denoted as R^* and is obtained from solving Algorithm 2 and compared with SOS and DAL estimates for the WKH and 9-state Couette flow models, respectively. The DAL method solves a variational problem for the nonlinear optimal perturbation, which is used as a benchmark for comparison. The SOS analysis uses the toolbox available in [20]. To solve Eq. (13) for the WKH model and 9-state models, we use 200 logarithmically spaced values of α between 10^{-5} and 10^{1}. We compute the ROA estimate using the largest radius obtained on this grid, i.e., $R^* := \max_i R(\alpha_i^*)$. The results in Figure 4 show that the ellipsoidal sets improve the estimates of $\hat{\mathcal{R}}_R$ compared to the spherical sets given in [12], [13]. This is true even at the initial iterate, which yields improvements of approximately 4 times and 2.5 times for the WKH and 9-state models, respectively. Additional refinement iterations improve the results even further. However we set the tolerance for convergence to 10^{-4}, and also observe only a marginal improvement after

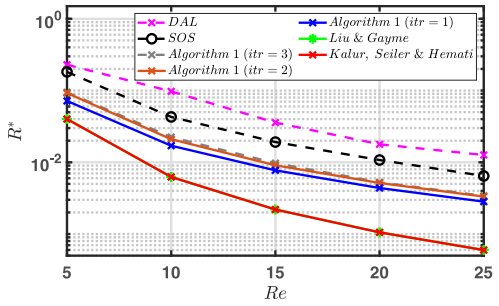

(a) WKH Model

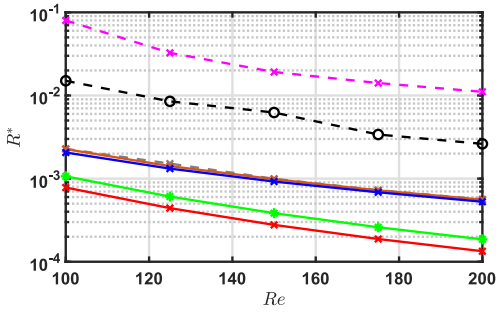

(b) 9-state Couette Flow Model

Fig. 4. The inner estimates of ROA obtained using Algorithm 1 show improved estimates compared to methods based on spherical sets.

three iterations of Algorithm 1 (gray curve). For the 9-state model, there is an improvement factor of roughly 2.4 and 3.3 using Algorithm 1 (blue curve) over the QC methods of Liu and Gayme and Kalur *et al.* Additionally, the improvement factor of R^* is ≈ 3.38 using Algorithm 1 as compared to the other two QC constraints for the WKH model.

In Figure 4, we also compare the results obtained using Algorithm 1 with SOS and DAL methods. We find that each iteration of Algorithm 1 reduces the conservatism of the QC estimates, but the inner estimate is still conservative relative to the SOS and DAL methods. More specifically, the largest radius R^* obtained from the SOS (black dashed curve) method and Algorithm 1 with 1 iteration (blue curve) differ by an average factor of ≈ 2.45 and ≈ 6.1 for the WKH and 9-state models, respectively. The differences in the R^* estimates become even greater for the DAL approach, with the DAL estimates (magenta curve) being larger by a factor of ≈ 3.5 and ≈ 23 than the Algorithm 1 estimates for the WKH and 9-state models, respectively. We note that SOS and DAL methods provide superior estimates of R^* because both of these methods use precise information of the nonlinearity and exact equations of motion. This is in contrast to the QC-based approaches, whereby only input-output properties of the nonlinear terms are used.

Next, we assess estimates of R^* using Algorithm 2 (see Figure 5). The second step in Algorithm 2 avoids the computationally demanding step of solving over a grid of α, as is required in Algorithm 1. Instead, Algorithm 2 directly determines the best α for the given shape E and Lyapunov energy matrix P, and thus provides an efficient "one-shot" approach to

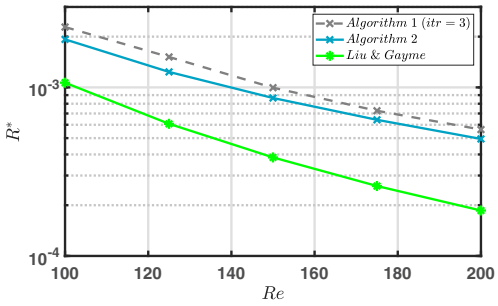

Fig. 5. The inner estimate of ROA obtained using Algorithm 2 for the 9-state model is conservative compared to the refinement using Algorithm 1.

estimate R^*. Since Algorithm 2 does not facilitate further iterations, in general it provides conservative results as compared to Algorithm 1. However, Algorithm 2 substantially reduces conservatism to prior formulations of the QC analysis presented in [12], [13]. In Figure 5, it can be seen that estimates from Algorithm 1 and 2 differ by a factor of roughly 1.16—on average—for the 9-state Couette flow model. Although not reported here, we made similar observations in our analysis of the WKH model, where the difference was roughly a factor of 1.06 between Algorithm 1 and 2 estimates of R^*.

Finally, we assess the computational run-time performance of the various methods investigated in this study. All computations were performed on an ASUS ROG M15 laptop with Intel 2.6 GHz i7-10750H CPU and a 16 GB RAM. Overall both Algorithm 1 and 2 proposed in this paper require less total run-time compared to DAL and SOS methods. This savings becomes especially apparent in analyzing the 9-state model. Although the SOS and DAL methods yield more accurate estimates, these methods scale poorly with the state dimension compared to the QC analysis methods. The SOS method for WKH has a wall-time of about 116.8 seconds as compared to 5.82×10^4 seconds for the 9-state model. Similarly, the solver run times for each iteration of WKH model is 2.9 seconds compared to 1.45×10^3 seconds for the 9-state model. Thus, in case of the SOS method, roughly doubling the states results in the total computation time increasing by a factor of $\approx$ 500. In contrast, the total run-time of the QC-based Algorithm 1 increased by a factor of roughly 20 between the 4-state WKH model and the 9-state model. For the 9-state model, when we compare the run-time for Algorithm 1 to the SOS method, we see that the QC method is approx 900 times faster. We note that the run-time for the DAL method appears to increase by a factor of roughly 15 when going from the 4-state WKH model to the 9-state model, which actually seems to scale better than even the QC method; however, it is important to note that the DAL method can be sensitive to the final simulation time, perturbation size, tolerances, etc. Thus, tuning the DAL method can be a time intensive process, especially when system parameters (e.g., Re) are changed. The time required to tune the DAL process to obtain the precise estimates reported in this study is not reflected in the times listed in Table I. Overall, we conclude that the QC-based Algorithms 1 and 2 require less end-to-end time than SOS

TABLE I
TOTAL RUN-TIME AND AVERAGE SOLVER TIME PER ITERATION FOR CALCULATING R^* BY THE VARIOUS METHODS STUDIED

Method	Run-time to convergence (secs)		Avg. solver time for one iteration (secs)	
	WKH	9-state	WKH	9-state
Algorithm 1 (solver: Mincx Matlab)	2.89	63.48	0.76×10^{-2}	0.15
Algorithm 2 (solver Mincx & gevp Matlab)	1.85	37.99	2.3×10^{-2}	0.49
DAL	9.82	137.6	8.64×10^{-4}	0.18×10^{-2}
SOS	116.8	5.82×10^{4}	2.9	1.45×10^{3}

and DAL methods, and yield R^* solutions that are approximately within one order of magnitude of the SOS and DAL estimates.

V. CONCLUSION

In this work, we have proposed an improvement to the quadratic constraint (QC) framework for nonlinear fluid flow analysis. This was done by generalizing the local QCs from spherical sets (proposed in [11]–[13]) to ellipsoidal sets, which reduced conservatism and improved estimates of the ROA. Additionally, we proposed and investigated two algorithms for performing the ROA analysis. The less conservative but more computationally demanding algorithm—Algorithm 1—iteratively refines the solution by solving a sequence of semi-definite programs. In contrast, the more computationally efficient algorithm—Algorithm 2—solves a single generalized eigenvalue problem (GEVP) and yields estimates of the ROA and permissible perturbation amplitude in a single pass. Both Algorithms 1 and 2 were found to outperform the QC analysis methods proposed in [12] and [13] in terms of accuracy. Algorithm 2 did so at no additional computational cost over these prior QC-based analysis methods. Both of the proposed algorithms surpassed prevailing SOS and DAL methods in terms of computational run-time. Although the proposed methods did not attain the same degree of accuracy as the computationally demanding SOS and DAL methods, both Algorithms 1 and 2 estimated results on the same order of magnitude as DAL and SOS for the models considered here. It may still be possible to refine the QC method beyond what we have presented in this study. Future work may benefit from incorporating additional constraints to refine the proposed QC analysis even further.

REFERENCES

[1] P. J. Schmid and D. S. Henningson, *Stability and Transition in Shear Flows*. New York, NY, USA: Springer, 2001.
[2] D. Barkley, "Theoretical perspective on the route to turbulence in a pipe," *J. Fluid Mech.*, vol. 803, p. 1, Sep. 2016.
[3] R. Kerswell, "Nonlinear nonmodal stability theory," *Annu. Rev. Fluid Mech.*, vol. 50, no. 1, pp. 319–345, 2018.
[4] H. K. Khalil, *Nonlinear Systems*, 3rd ed. Princeton, NJ, USA: Prentice-Hall, 2002.
[5] M. Ahmadi, G. Valmorbida, D. Gayme, and A. Papachristodoulou, "A framework for input-output analysis of wall-bounded shear flows," *J. Fluid Mech.*, vol. 873, pp. 742–785, Jun. 2019.
[6] S. Zhao and S. Duncan, "Passivity of plane poiseuille flow," in *Proc. Eur. Control Conf. (ECC)*, 2013, pp. 1077–1082.
[7] P. J. Goulart and S. Chernyshenko, "Global stability analysis of fluid flows using sum-of-squares," *Physica D, Nonlinear Phenomena*, vol. 241, no. 6, p. 692–704, Mar. 2012.
[8] D. D. Joseph, *Stability of Fluid Motions I*. Heidelberg, Germany: Springer-Verlag, 1976.
[9] F. Amato, C. Cosentino, and A. Merola, "On the region of attraction for nonlinear quadratic systems," *Automatica*, vol. 43, pp. 2119–2123, Dec. 2007.
[10] F. Amato, C. Cosentino, and A. Merola, "On the region of asymptotic stability of nonlinear quadratic systems," in *Proc. 14th Mediterr. Conf. Control Autom.*, vol. 1, 2006, pp. 1–5.
[11] A. Kalur, P. Seiler, and M. Hemati, "Stability and performance analysis of nonlinear and non-normal systems using quadratic constraints," in *Proc. AIAA Aerosp. Sci. Meeting*, Jan. 2020, Art. no. 0833.
[12] A. Kalur, P. Seiler, and M. S. Hemati, "Nonlinear stability analysis of transitional flows using quadratic constraints," *Phys. Rev. Fluids*, vol. 6, Apr. 2021, Art. no. 044401.
[13] C. Liu and D. F. Gayme, "Input-output inspired method for permissible perturbation amplitude of transitional wall-bounded shear flows," *Phys. Rev. E*, vol. 102, Dec. 2020, Art. no. 063108.
[14] F. Waleffe, J. Kim, and J. M. Hamilton, "On the origin of streaks in turbulent shear flows," in *Turbulent Shear Flows 8*. Heidelberg, Germany: Springer, 1993, pp. 37–49.
[15] J. Moehlis, H. Faisst, and B. Eckhardt, "A low-dimensional model for turbulent shear flows," *New J. Phys.*, vol. 6, p. 56, May 2004.
[16] F. Waleffe, "Transition in shear flows. Nonlinear normality versus non-normal linearity," *Phys. Fluids*, vol. 7, no. 12, pp. 3060–3066, 1995.
[17] S. Boyd, L. El Ghaoui, E. Feron, and V. Balakrishnan, *Linear Matrix Inequalities in System and Control Theory*, vol. 15. Philadelphia, PA, USA: Soc. Ind. Appl. Math., 1994,
[18] S. Boyd and L. Vandenberghe, *Convex Optimization*. Cambridge, U.K.: Cambridge Univ. Press, 2004.
[19] S. Boyd and L. E. Ghaoui, "Method of centers for minimizing generalized eigenvalues," *Linear Algebra Appl.*, vols. 188–189, pp. 63–111, Jul./Aug. 1993.
[20] G. Balas, A. Packard, P. Seiler, and U. Topcu. *Robustness Analysis for Nonlinear Systems*. Accessed: Jun. 4, 2020. [Online]. Available: https://dept.aem.umn.edu/~AerospaceControl/